

Effect of Transition Metal/Graphitic Carbon Nitride for Photoreduction of Hexavalent Chromium

M.S. Azami^{1,*}, A.R. Faatihah¹, A.H. Nordin¹, K.H. Tan², N. Jamaluddin³, N.M. Izzudin⁴, A.A. Azmi⁵

¹ Faculty of Applied Sciences, Universiti Teknologi MARA, 02600 Shah Arau, Perlis, Malaysia

² Centre for Advanced Materials, Faculty of Engineering and Technology, Tunku Abdul Rahman University of Management and Technology, 53300 Kuala Lumpur, Malaysia

³ Faculty of Science, Universiti Teknologi Malaysia, 81310 UTM Johor Bahru, Johor, Malaysia

⁴ School of Chemical and Energy Engineering, Faculty of Engineering, Universiti Teknologi Malaysia, 81310 UTM Johor Bahru, Johor, Malaysia.

⁵ Graduate School of Science and Engineering, Saga University, 1 Chome Honjomachi, Saga, 840-8502, Jepun

*Corresponding Author: saifulddin@uitm.edu.my

Article history:

Received 13 November 2023

Accepted 27 December 2023

ABSTRACT

Recently, the discharge of heavy metals such as hexavalent chromium (Cr (VI)) into water is increasing due to the development of industrials. This poses a huge environmental challenges as toxic waste of heavy metal leads to water pollution which give a negative impact on health and environment. This heavy metal can be treated by reducing the highly poisonous of Cr (VI) to less toxic trivalent chromium Cr (III). Nowadays, the photocatalytic reduction is one of the effective methods that can reduce Cr (VI) to harmless toxic into the environment. In this study, the effect of different metal of Ag, Cu and Ni loaded on g-C₃N₄ were investigated based on the structural, morphological, compositional, and optical properties. The different metal of Ag, Cu and Ni were loaded on g-C₃N₄ by using impregnation method. The physical and chemical properties of Ag, Cu and Ni loaded on g-C₃N₄ were analyzed using FTIR and UV-vis/DRS techniques. The performance of photocatalytic activity among Ag, Cu and Ni loaded on g-C₃N₄ were evaluated for photoreduction of Cr (VI) and the highest performance of photoreduction of Cr (VI) was demonstrated by Ag/C₃N₄ (87%), followed by Cu/C₃N₄ (85%), Ni/C₃N₄ (80%) and pure g-C₃N₄ (77%) under visible-light. Among of photocatalyst, Ag/C₃N₄ was revealed as the best performance in photoreduction of Cr (VI) owing to its change in morphology, strong interaction between Ag and C N bonds and low band gap. Besides, the effect of scavengers shows the active species was the photogenerated electron (e⁻) play an important role on photoreduction of Cr (VI). Overall, the Ag loaded on g-C₃N₄ was successfully contribute on photoreduction of Cr (VI) under visible light.

Keywords: Hexavalent chromium, Transition metal, Graphitic carbon nitride, Photocatalyst, Impregnation method

© 2023 Faculty of Chemical and Engineering, UTM. All rights reserved
| eISSN 0128-2581 |

1. INTRODUCTION

The exposure of the Cr (VI) can cause high detrimental to human body including asthma, eye irritation and damage, perforated eardrums, respiratory irritation, kidney damage, liver damage, pulmonary congestion and edema, upper abdominal pain, nose irritation and damage, respiratory cancer, skin irritation, and erosion and discoloration of the teeth [1]. Therefore, many efforts have been done to reduce the Cr (VI) into Cr (III) by using electrocoagulation, biosorption, ion exchange, adsorption, and electrochemical reduction [2,3]. Unfortunately, these methods have several drawbacks such as costly in setup the treatment reactor, consuming a lot of time in treatment

process, potential to produce secondary product and sewage sludge production [4].

The alternative approach to reduce Cr (VI) is by using photocatalytic reduction method due to its low cost, easy operation, and excellent safety [5]. By doing so, the extremely toxic Cr (VI) can be reduced to less toxic Cr (III) which is a trace element need by humans and easily precipitated in aqueous medium [5]. Graphitic carbon nitride (g-C₃N₄) is good potential photocatalyst for environmental remediation. The g-C₃N₄ is a non-metal-based semiconductor photocatalyst that has been extensively explored because of its non-toxicity, inexpensive cost, visible-light driven, narrow band gap, and great stability [6]. Furthermore, when compare to reduction potential of Cr (VI) to Cr (III), the conduction band of g-C₃N₄ is more negative,

indicated that the photo-generated electrons of g-C₃N₄ have a high thermodynamic driving force to cause a reduction of Cr (VI) into Cr (III) [7]. However, there are some disadvantages of using g-C₃N₄ such as low utilization rate of visible-light, rapid recombination of electron hole pairs, and small specific surface area [8]. In recent research, transition metal has been shown a good potential to overcome these issues and therefore, enhance the photocatalytic activity of g-C₃N₄. This is because, the presence of transition metals inhibited the recombination of electron-hole and enhanced the visible light absorption [9]. Therefore, it is an effective strategy to improve the application of g-C₃N₄ under visible light as it modifies the structure of the electronic band gap by metal doping [10].

In this study, the different transition metals such as Ag, Cu and Ni have been chosen to be loaded on g-C₃N₄ to enhance the photoreduction of Cr (VI). The presence of metal on g-C₃N₄ could formed new energy levels, extended the visible light response, and suppressed the electron-hole charge recombination rate [11]. Then, physical, and chemical properties of Ag, Cu and Ni loaded on g-C₃N₄ were investigated using FTIR and UV-vis/DRS in order to identify the functional group and optical properties of the prepared photocatalysts, respectively which can be correlated with the photocatalytic performance of photoreduction Cr (VI).

2. EXPERIMENTS

2.1 Preparation of g-C₃N₄

The g-C₃N₄ was synthesized by using urea under heat treatment method. 10 g of urea was placed into an alumina crucible and was covered with lid. Then the sample was calcined at 550 °C for 3 hours in air (5 °C/min) to obtained yellow colour of g-C₃N₄.

2.2 Preparation of Transition Metals Loaded on g-C₃N₄

The Ag, Cu and Ni loaded on g-C₃N₄ were prepared by using impregnation method. Firstly, 0.1 g of g-C₃N₄ was added into 25 mL of H₂O and stirred for 10 minutes. Then, 0.5 wt.% of AgNO₃ dissolved in 25 mL of H₂O was mixed into the g-C₃N₄ solutions. After that, the solution was stirred for 30 minutes at 50 °C and continuously stirred until dried at 80 °C. Next, the mixture was further dried in an oven at 100 °C for 3 hours. Finally, the sample was calcined at 550 °C for 3 hours and denoted as Ag/ g-C₃N₄. A similar procedure was repeated by using others metal precursor (Copper (II) Nitrate Trihydrate and Nickel (II) Sulfate Hexahydrate) loaded on g-C₃N₄, which denoted as Cu/g-C₃N₄ and Ni/g-C₃N₄ respectively.

2.3 Characterization of The Prepared Photocatalysts

The chemical composition analysis was examined using Fourier transform infrared (FTIR) via KBR method (Agilent with model instrument Cary 640), The absorbance of optical properties for the prepared photocatalysts was determined using (Agilent Cary 60) ultraviolet-visible/diffuse reflectance spectra (UV-Vis/DRS) spectrophotometer.

2.4 Photocatalytic Reduction of Cr (VI)

The photocatalytic activity of Ag/C₃N₄, Cu/C₃N₄ and Ni/C₃N₄ photocatalysts were investigated for reduction of Cr(VI) under visible light. The 300 W xenon lamp was used as radiant source. The prepared photocatalyst was added (0.0094 g) to the mixture of 25 mL of K₂Cr₂O₇, 1 mL of diphenylcarbazide solution (indicator) and a drop of H₂SO₄. The concentration of Cr(VI) was measured using 1,5-diphenylcarbazide (DPC) method which the sample's absorbance was measured at 540 nm by carried out using UV-Vis spectrophotometer. The solution was stirred for 15 minutes in the absence of a light source to achieve adsorption-desorption equilibrium between the catalyst and Cr (VI) and to determine the adsorption equilibrium time. After 15 min in the dark, the lamp was turned on to start the photocatalytic reaction. Then, 3.0 mL of sample of Cr (VI) solution was collected and centrifuged for 15 minutes.

3. RESULTS AND DISCUSSION

3.1 Characterization of Photocatalyst

The optical properties for prepared photocatalysts were determined by UV/Vis DRS as depicted in Figure 1. Figure 1 (a) shows the UV-vis DRS analysis of the pure g-C₃N₄, Ag/C₃N₄, Cu/C₃N₄, and Ni/C₃N₄ at range of 200-800 nm. Figure 1 (b) shows the bandgap energy of each photocatalyst which converted from Kubelka-Munk equation. Based on the result, the steeper curve of Ag/C₃N₄ shows large absorption band in the visible light region compared to pure g-C₃N₄. The optical band edge of g-C₃N₄ was observed at 480 nm. The absorbance of Ag/C₃N₄ extended further in the visible range of g-C₃N₄ is extrapolated at 500 nm. The shift of Ag/C₃N₄ indicate a potential of strong interaction between the C, N and Ag bonds that improve the efficiency of charge separation which enhance the activity of photoreduction [12]. Thus, Ag/C₃N₄ form more electron-hole pairs and absorb more photons can also give a significant performance on photoreduction of Cr (VI). Furthermore, the bandgap energy of g-C₃N₄, Ag/C₃N₄, Cu/C₃N₄ and Ni/C₃N₄ were determined to be 2.70, 2.60, 2.65 and 2.68 eV, respectively. Ag/C₃N₄ shows the lowest bandgap energy followed by Cu/C₃N₄, Ni/C₃N₄ and pure g-C₃N₄. The doped metal especially Ag/C₃N₄ shows the improvement in visible light absorption, decrease the recombination rate of electron-hole pairs as its reduce in the bandgap energy [13].

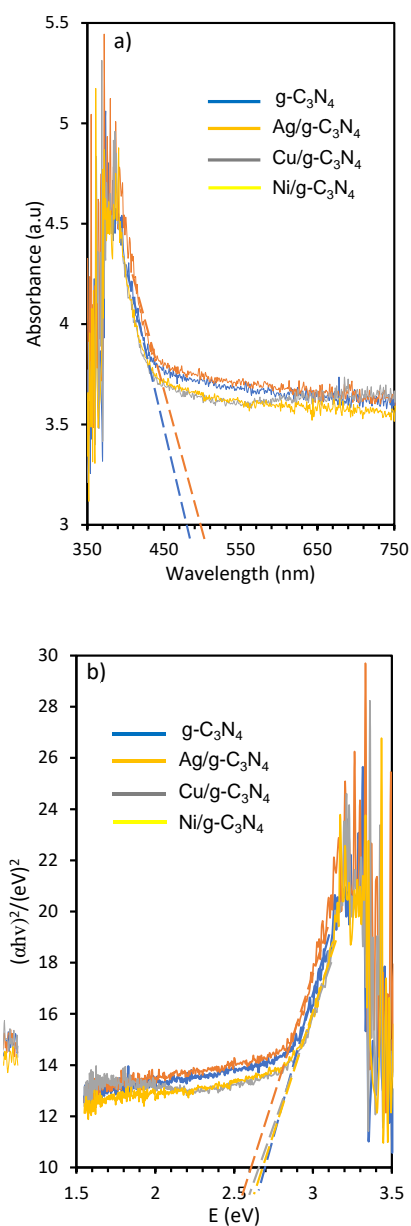


Figure 1. (a) UV-vis diffuse reflectance spectra (b) Plot of transformed Kubelka-Munk function versus energy of light for the prepared photocatalysts

The FTIR analysis was carried out to determine the functional groups present in g-C₃N₄, Ag/C₃N₄, Cu/C₃N₄ and Ni/C₃N₄ with the range of 400-4000 cm⁻¹ as shown in Figure 2. In the pure g-C₃N₄ photocatalyst (Figure 2 (d)), the vibrational broad peak shows at 3176.46 cm⁻¹ indicate the present of N-H bond stretching associated with uncondensed amino groups and surface adsorbed water molecules [13]. The peaks at 1549.04 cm⁻¹ to 1622.09 cm⁻¹ corresponds to stretching mode of the C=N bond [14]. Meanwhile, the strong peaks observed in the region 1403.32 cm⁻¹ can be attributed to the presence of aromatic of C-N heterocycles [15]. Then, the peak at 1234.19 cm⁻¹ can be assigned to stretching vibrations of C-N-C or bridging C-NH-C bonds.

The sharp peak at 806.11 cm⁻¹ can be assigned to the s-triazine (heptazine) ring vibrations [16]. These peak indicate the synthesized of g-C₃N₄ is composed of heptazine units.

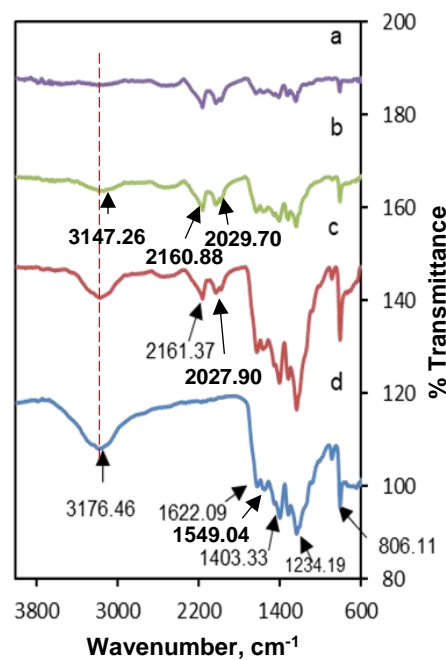


Figure 2. FTIR spectra of synthesized (a) Ni/C₃N₄, (b) Cu/C₃N₄, (c) Ag/C₃N₄ and (d) g-C₃N₄

Based on the FTIR, all the characteristic of vibrational peaks related to g-C₃N₄ can be observed in Ag/C₃N₄ photocatalyst (Figure 2(c)). This result showed that after modification of photocatalysts the structure of g-C₃N₄ is remained unchanged. However, the absorption peaks of N-H bonds gradually decrease with the additional of Ag doping. This is because of Ag⁺ can be anchored to amino groups through complexation and redox, then being photo-reduced to Ag⁰ during photo-deposition process [17]. As a result, Ag nanoparticles form around the amino groups and interfere the stretching vibration of N-H bonds. Next, a peak at 2027.90 cm⁻¹ and 2161.37 cm⁻¹ is clearly observed in the Ag/C₃N₄ spectra but not in g-C₃N₄. This peak is attributed to the Ag-N stretching mode, indicating that silver atoms were successfully doped into the g-C₃N₄ crystal lattice [17]. Meanwhile, the stretching vibration frequencies of Cu/C₃N₄ differ slightly from pure g-C₃N₄ as can be seen in Figure 2 (b). The main absorption peak of N-H in the Cu/C₃N₄ composite at 3147.26 cm⁻¹, indicating that there is not much shifted in the absorption peak position. However, it indicates that copper was successfully loaded onto g-C₃N₄, although the characteristics did not change much since Cu-N stretching mode appear at 2029.70 and 2160.85 cm⁻¹ [18]. Meanwhile, Ni/C₃N₄ also shows slightly different from the pure g-C₃N₄. The main characteristic peak of the C=N (1575.60 and 1637.4 cm⁻¹) and C-N (1320.1 and 1410.95 cm⁻¹) stretching vibration frequency of the metal doped g-C₃N₄ was higher than the pure g-C₃N₄ as shown in Figure

2(a). The shifting of the C=N and C–N stretching frequencies are due to coordination of metal ions with the nitrogen atom in the g-C₃N₄.

3.2 Photocatalytic Performance

The photocatalytic activity performance of Ag, Cu and Ni loaded on g-C₃N₄ catalysts on the photoreduction of Cr (VI) were conducted under the visible light irradiation (Figure 3). It is observed that Ag/C₃N₄ (87%) is the most effective photocatalyst on photoreduction of Cr (VI) followed by Cu/C₃N₄ (85%), Ni/C₃N₄ (80%) and pure g-C₃N₄ (77%). This indicates that the pure g-C₃N₄ photocatalyst doping with metal improved photocatalytic reduction of Cr (IV). The lowest performance by g-C₃N₄ could be attributed to high recombination of electron-hole pair [14]. Meanwhile, the improvement on photoreduction of Cr (VI) over Ag/C₃N₄ could be impacted due to the high interaction between Ag and g-C₃N₄ with lowest bandgap (2.60 eV) as compared with others prepared photocatalyst, which enhanced the absorption of visible light.

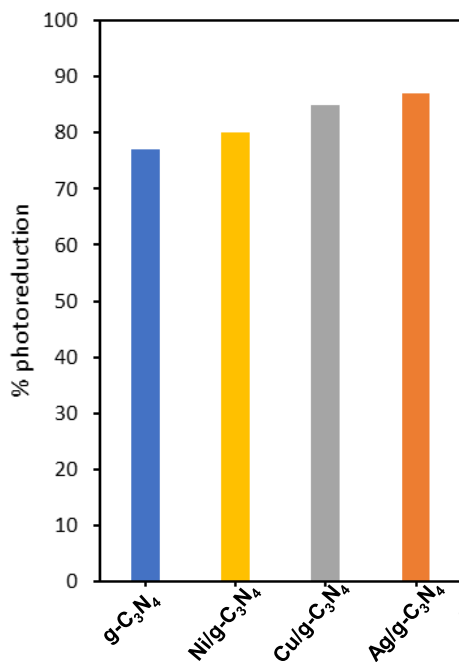


Figure 3. Photoreduction of Cr(VI) using pure g-C₃N₄, Ni/C₃N₄, Cu/C₃N₄ and Ag/C₃N₄ under visible light irradiation ((C_{Cr(VI)})=10 mg L⁻¹, pH = 5, W = 0.375 g L⁻¹, t = 90 min)

3.3 Photoreduction Mechanism

The proposed mechanism for photoreduction of Cr (VI) was deduced by investigating the respective impact of photoactive radical species on the reaction. The effect of scavenger was performed to determine the role of scavenger species in the photocatalytic mechanism of Cr (VI) over

Ag/C₃N₄. According to Figure 4, the photoreduction of Cr (VI) using Ag/C₃N₄ without scavenger species shows the best performance compared with the presence of scavenger. The experiment was examined by using Potassium Chlorate (PC) and Methanol (ME) as scavenger species for photogenerated electrons (e⁻) and photogenerated holes (h⁺) respectively. The scavengers determine that photogenerated e⁻ (70%) followed by photogenerated h⁺ (72%) which shows slightly decrease in the performance of photoreduction of Cr (VI). Based on the result, the crucial active species was photogenerated e⁻ because of the lowest performance compared to h⁺. Moreover, results indicate that the interaction of Ag on g-C₃N₄ show a significant contribution on photoreduction of Cr (VI) under visible light.

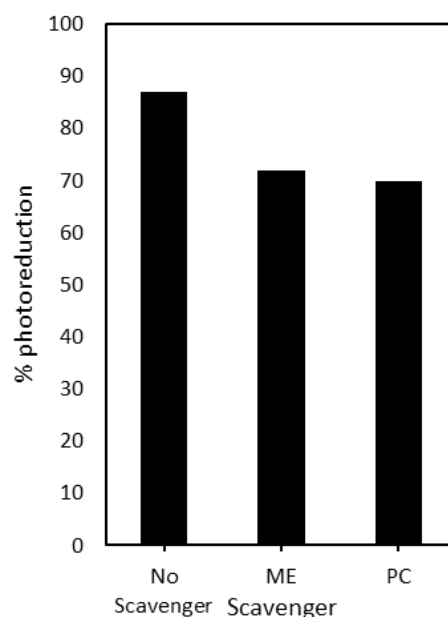


Figure 4. Photoreduction of Cr (VI) in the presence of scavenger using Ag/C₃N₄ photocatalyst (C_{Cr(VI)})=10 mg L⁻¹, pH = 5, W = 0.375 g L⁻¹, t = 90 min)

Figure 5 depicts the proposed of illustrated Ag/C₃N₄ mechanism. According to the effect of scavenger for Ag/C₃N₄, the photogenerated e⁻ and h⁺ species shows favourable for the formation of a Schottky junction. The e⁻ was moved leaving h⁺ from the valence band (VB) to the conduction band (CB) of g-C₃N₄. However, previous research reported the value of VB for g-C₃N₄ was about 1.23 eV. Noticeably illustrated that h⁺ is incapable of converting H₂O to •OH because the potential level of •OH was 2.44 eV which higher compared to level of VB. Next, photogenerated e⁻ then move to Ag from CB of g-C₃N₄. The effectiveness of electromagnetic field may be improved by the Ag effect on the surface plasmonic resonance (SPR) because it potentially accelerates the rate of photogenerated electron-holes generation. As a result, the photogenerated e⁻ can react with O₂ to form •O₂⁻. This species is in charge of increasing activity on photoreduction Cr (VI). Therefore, the mechanism described above show that the loading of Ag on g-C₃N₄ was generate a Schottky junction. Schottky junction

photocatalyst demonstrates how the interaction of Ag and g-C₃N₄ increased the electron generated and play as a catalyst for more effectively capturing light and transferring charge, hence increase the activity on photoreduction of Cr (VI).³

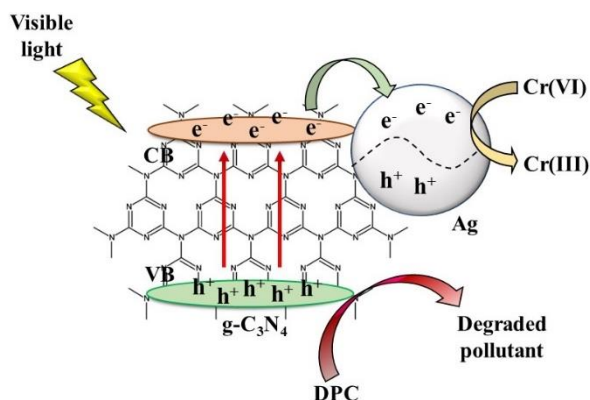


Figure 5. Mechanism of photocatalytic activity of Ag/C₃N₄.

4. CONCLUSION

g-C₃N₄ was prepared using urea as a precursor and loaded with metal using impregnation method to enhance the photoreduction activity. The physical and chemical properties of the photocatalysts were examined using, FTIR and UV-Vis DRS. The highest performance of photoreduction of Cr (VI) was demonstrated by Ag/C₃N₄ (87%), followed by Cu/C₃N₄ (85%), Ni/C₃N₄ (80%) and pure g-C₃N₄ (77%) under visible-light. Among of photocatalyst, Ag/C₃N₄ was revealed as the best performance in photoreduction of Cr (VI) due to strong interaction between Ag and C, N bonds and low band gap. Moreover, the effect of scavenger shows the active species was the photogenerated electron (e⁻) play an important role on photoreduction of Cr (VI). Overall, the Ag loaded on g-C₃N₄ was successfully contribute on photoreduction of Cr (VI) under visible light.

ACKNOWLEDGEMENTS

The authors are grateful for the financial support by the Research University Grant from Universiti Teknologi MARA (Grant No. PY/2023/00444).

REFERENCES

1. Wu, J. H., Shao, F. Q., Han, S. Y., Bai, S., Feng, J. J., Li, Z., & Wang, A. J., *Journal of Colloid and Interface Science*, **535** (2019) 41–49. <https://doi.org/10.1016/j.jcis.2018.09.080>
2. Hasija, V., Raizada, P., Singh, P., Verma, N., Khan, A. A. P., Singh, A., Selvasembian, R., Kim, S. Y., Hussain, C. M., Nguyen, V. H., & Le, Q. Van.

3. Process Safety and Environmental Protection, **152** (2021).663–678. <https://doi.org/10.1016/j.psep.2021.06.042>.
4. Liu, S., Zhang, W., Zhu, P., Zuo, S., & Xia, H. *Journal of Environmental Chemical Engineering*, (2021). <https://doi.org/10.1016/j.jece.2021.105879>.
4. Azami, M. S., Jalil, A. A., Aziz, F. F. A., Hassan, N. S., Mamat, C. R., Fauzi, A. A., & Izzudin, N. M., *Separation and Purification Technology*, 292 (2022) 120984. <https://doi.org/10.1016/j.seppur.2022.120984>.
5. Islam, J. B., Furukawa, M., Tateishi, I., Katsumata, H., & Kaneco, S., *ChemEngineering*, 3 (2019) 1–10. <https://doi.org/10.3390/chemengineering302003>.
6. Lin, H., Wu, J., Zhou, F., Zhao, X., Lu, P., Sun, G., Song, Y., Li, Y., Liu, X., & Dai, H., *Journal of Environmental Sciences*, **124** (2021) 570–590. <https://doi.org/10.1016/j.jes.2021.11.017>.
7. Barolo, G., Livraghi, S., Chiesa, M., Paganini, M.C., Giamello, E., *Journal of Physical Chemistry*. (2012) 20887–20894.
8. Orlando C-Neto and Maurício S. B., *Cosmetoscope*. **21** (2015) 4.
9. Prabakaran, E., & Pillay, K., *ACS Omega*, **6** (2021) 35221–35243. <https://doi.org/10.1021/acsomega.1c00866>
10. Viet, N. M., Trung, D. Q., Giang, B. L., Tri, N. L. M., Thao, P., Pham, T. H., Kamand, F. Z., & Al Tahtamouni, T. M., *Journal of Water Process Engineering*, **32** (2019) 100954. <https://doi.org/10.1016/j.jwpe.2019.100954>
11. Jiang, L., Yuan, X., Pan, Y., Liang, J., Zeng, G., Wu, Z., & Wang, H., *Applied Catalysis B: Environmental*, **217** (2017) 388–406. <https://doi.org/10.1016/j.apcatb.2017.06.003>
12. Yan, W., Yan, L., & Jing, C. *Applied Catalysis B: Environmental*, **244** (2019) 475–485. <https://doi.org/10.1016/j.apcatb.2018.11.069>
13. Zhang, Y., Yuan, J., Ding, Y., Liu, B., Zhao, L., & Zhang, S., *Ceramics International*, **47** (2021) 31005–31030. <https://doi.org/10.1016/j.ceramint.2021.08.063>
14. Azami, M. S., Jalil, A. A., Nawawi, W. I., Mamat, C. R., & Izzudin, N. M., *Materials Today: Proceedings*, **66** (2022) 4068–4072.
15. Durairaj, A., Sakthivel, T., Obadiah, A., & Vasanthkumar, S., *Journal of Materials Science: Materials in Electronics*, **29** (2018) 8201–8209. <https://doi.org/10.1007/s10854-018-8826-5>.
16. Faisal, M., Ismail, A. A., Harraz, F. A., Al-Sayari, S. A., El-Toni, A. M., & Al-Assiri, M. S. *Materials and Design*, **98** (2016) 223–230. <https://doi.org/10.1016/j.matdes.2016.03.019>
17. Hayat, A., Al-Sehemi, A. G., El-Nasser, K. S., Taha, T. A., Al-Ghamdi, A. A., Jawad Ali Shah Syed, Amin, M. A., Ali, T., Bashir, T., Palamanit, A., Khan, J., & Nawawi, W. I., *International Journal of Hydrogen Energy*, **47** (2022), 5142–5191.